

Adaptive Spatial Resampling Applied to Seismic Inverse Modeling

Cheolkyun Jeong¹, Tapan Mukerji² and Gregoire Mariethoz³

Abstract Seismic inverse modeling, which transforms obtained geophysical data into physical properties of the Earth, is an essential process for reservoir characterization. We propose a Markov chain Monte Carlo (McMC) workflow consistent with geology, well-logs, seismic data and rock-physics information. The workflow uses Direct Sampling (DS), a multiple-point geostatistical method, for generating realizations from the prior distribution and Adaptive Spatial Resampling (ASR) for sampling from the posterior distribution conditioned to the geophysical data. Sampling is a more general approach than optimization as it can assess important uncertainties and not just the most likely model. However, since rejection sampling requires a large number of evaluations of forward model, it is inefficient and not suitable for reservoir modeling. Metropolis sampling is able to perform a reasonably equivalent sampling by forming a Markov chain. The ASR algorithm perturbs realizations of a spatially dependent variable while preserving its spatial structure by conditioning to subset points. The method is used as a transition kernel to produce a Markov chain of geostatistical realizations. These realizations are then used in a forward seismic model to compute the predicted data which are compared to the observed data. Depending on the acceptance/rejection criterion in the Markov process, it is possible to obtain a chain of realizations aimed either at characterizing the posterior distribution with Metropolis sampling or at calibrating a single realization until an optimum is reached. Thus the algorithm can be tuned to work either as an optimizer or as a sampler. The validity and applicability of the proposed method is demonstrated by results for seismic lithofacies inversion on a synthetic test set of Stanford VI.

Cheolkyun Jeong¹ Stanford University, 367 Panama St #65, Stanford, CA94305, USA
email : ckjeong@stanford.edu

Tapan Mukerji² Stanford University, 367 Panama St #65, Stanford, CA94305, USA
email : mukerji@stanford.edu

Gregoire Mariethoz³ University of New South Wales, UNSW 2052, Sydney, Australia
email: gregoire.mariethoz@unsw.edu.au

1. Introduction

Seismic data play a key role to reduce uncertainty in predictions of rocks and fluids away from well control points. However, in real applications it is nearly impossible to find a unique relationship between seismic response and reservoir properties. Seismic measurements are noisy and have larger scales of resolution than well data. Moreover, the relationships are non-unique due to the limited frequency of seismic waves, the forward modeling simplifications, and natural heterogeneity.

Statistical rock physics accounts for some of the uncertainty using multi-variate stochastic relations between elastic parameters and reservoir properties [2, 12, and 13]. Many different workflows have been suggested to combine rock physics and geostatistical methods in seismic inversion. Bosch et al. [5] classified these approaches into two groups, which are the sequential or cascaded approach and the joint or simultaneous workflow in a Bayesian formulation. The joint or simultaneous workflow accounts for the elastic parameters and the reservoir properties together and provides combined uncertainties. These Bayesian workflows include rock-physics relations to link reservoir properties and elastic properties and geostatistical models to provide geologically consistent prior models. Forward modeled synthetic data are compared with obtained seismic data to calculate the likelihood, and the final solutions are posterior models consistent with the expected geology, well data and seismic data. Gonzalez et al. [7] combined multiple points geostatistics (MPS) and rock physics for seismic inversion. They generate multiple realizations of reservoir facies and saturations, conditioned to seismic and well data. MPS is used to characterize the geologic prior information, and statistical rock physics links reservoir properties to elastic properties. Thus their method provided multiple realizations, all consistent with the expected geology, well-log, seismic data and local rock-physics transformations. However, this workflow did not produce samples of the full posterior probability density function but generated multiple optimized models around the mode of the posterior. Also the MPS algorithm was inefficient for applying to 3-D and complicated actual field cases.

In posterior sampling methods, rejection sampler [16] is the only one to rigorously sample the posterior pdf. However, since it requires a large number of evaluations of forward model, rejection sampling is inefficient. Therefore, a key issue is to generate prior models and to find the posterior models honoring both spatial constraints and seismic data within limited computation time and cost.

We propose a Markov chain Monte Carlo (McMC) workflow consistent with geology, well-logs, seismic data and rock-physics information. The workflow uses Direct Sampling (DS), a multiple-point geostatistical method, for generating realizations from the prior distribution and Adaptive Spatial Resampling (ASR) for

sampling from the posterior distribution conditioned to the geophysical data. Since the conventional MPS algorithms such as SNESIM or SIMPAT store all data events from the training image [1, 14], computing load is dramatically increased according to the size of the template and the number of facies. The DS algorithm [9] characterizes the geological prior information and is used to condition to well data. The DS algorithm directly samples the training image for any given data event, without storing all patterns in a database. Therefore, less memory intensive DS can reproduce the structures of complex training images and deal with a wide range of non-stationary problems. The ASR algorithm perturbs realizations of a spatially dependent variable while preserving its spatial structure. The method is used as a transition kernel to produce a Markov chain of geostatistical realizations. These realizations are then used in a forward seismic model to compute the predicted data which are compared to the observed data. Depending on the acceptance/rejection criterion in the Markov process, it is possible to obtain a chain of realizations aimed either at characterizing the posterior distribution with Metropolis sampling or at calibrating a single realization until an optimum is reached. Thus the algorithm can be tuned to work either as an optimizer or as a sampler. The proposed method is demonstrated on a synthetic test dataset.

2. Methodology

2.1. Seismic inverse modeling in a Bayesian frame

The transformation of geophysical data into reservoir properties can be posed as an inference problem involving the updating of prior knowledge with newly available data [15, 16]. It can be expressed as

$$P_{post}(m) = cP_{prior}(m)P_{data}(d_{obs} - g(m)), \quad (1)$$

where $P_{post}(m)$ is the posterior probability density and $P_{prior}(m)$ is a priori probability density. In Equation (1), c is a normalizing constant, and m is the earth model parameter configuration. The expression $P_{data}(d_{obs} - g(m))$ is the data-likelihood function; and it depends on the observations d_{obs} and their uncertainty, and the forward modeling operator g that maps the model space into the data space. The solutions of an inverse problem are the set of earth-model configurations that, when forward modeled into synthetic data, match the real data within some tolerance [5].

According to the chain rule (see e.g., [3, 4]), decomposing the model space into reservoir parameters (facies, porosity, etc.) and elastic parameters [seismic velocity (V_p , and V_s), and density] the prior can be written as:

$$P_{prior}(m_{res}, m_{elas}) = P_{prior}(m_{elas}|m_{res})P_{prior}(m_{res}), \quad (2)$$

where $P_{prior}(m_{res})$ is the prior pdf for the reservoir parameters (including their spatial distributions) and $P_{prior}(m_{elas}|m_{res})$ is a conditional probability for the elastic parameters that summarizes the rock physics relationships between reservoir property and elastic property. Thus, the final posterior pdf for the joint rock physics and seismic inversion is the following combination of Equation (1) and (2):

$$P_{post}(m_{res}, m_{elas}) = c P_{prior}(m_{elas}|m_{res})P_{prior}(m_{res})P_{data}(d_{obs} - g(m_{elas})). \quad (3)$$

The petrophysical conditional density $P_{prior}(m_{elas}|m_{res})$ is the rock physics forward function that maps the reservoir model parameters to the elastic model parameters. Many different seismic inversion workflows combining elastic properties, geostatistics, and rock-physics models to predict reservoir properties can be presented in the shape of Equation (3) (Figure 1). This workflow in a Bayesian formulation guarantees consistency between the elastic and reservoir properties.

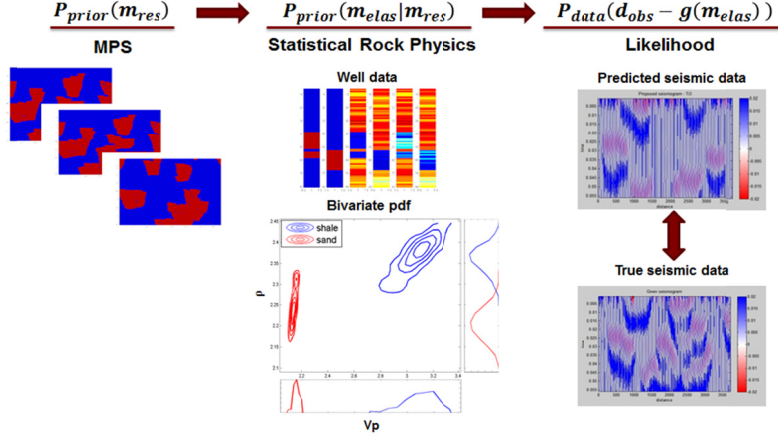


Figure 1 (left) Multiple models are generated by multiple-points geostatistics as priors, and (middle) the facies models are converted to V_p and density according to the rockphysics relationship in the bivariate pdf. (right) To falsify incorrect models, predicted seismograms are compared to the obtained seismic data. Here we assumed seismic forward modeling without noise and applied 50 (Hz) as a signal frequency.

2.2. Sampling posteriors

2.2.1. Rejection sampling

Sampling the posteriors is more important than a single optimization result but it takes tremendous time and cost. These problems are critical especially in complex models such as an actual reservoir case. Tarantola [16] gives a comprehensive overview of the available exact methods to obtain representative samples of $P_{post}(m|d)$. Rejection sampling is based on the fact that the posterior is a subset of the prior distribution, and therefore it can be evaluated by sub-sampling the prior. The approach consists in generating candidate models m^* that are samples of $P_{prior}(m)$ and to accept each of them with a probability in Equation (4)

$$P(m^*) = \frac{L(m^*)}{L(m)_{max}}, \quad (4)$$

where $L(m)_{max}$ denotes the supremum, which can be any number equal or above the maximum likelihood value that can be taken by $L(m)$. The distribution of the resulting samples follows posterior distribution of models. Rejection sampling is the only method perfectly falsifying incorrect priors. However, since it requires a large number of evaluations of $P_{prior}(m)$, the rejection method is inefficient.

2.2.2. Iterative spatial resampling

The Metropolis algorithm [10] is able to perform a reasonably equivalent sampling by forming a Markov chain of models, such that the steady-state distribution of the chain is precisely the posterior distribution that one wishes to sample from. It is similar to a random walk that would preferentially visit the areas where $P_{post}(m|d)$ is high. Specifically in reservoir modeling, the issue is how to form and perturb a Markov chain while preserving spatial structure of geomodels in the chain. One way is to sample a subset of points from previous model in a chain, and use the points as conditioning data for the next simulated realization.

Mariethoz et al. [8] suggested the Iterative Spatial Resampling (ISR) method to perturb realizations of a spatially dependent variable while preserving its spatial structure. This method is used as a transition kernel to produce Markov chains of geostatistical realizations.

Creating a Markov chain using ISR is accomplished by performing the following steps at each iteration i (Figure 2 and Figure 3):

- Generate m_1 and evaluate its likelihood, $L(m_1) = P_{data}(d_{obs} - g(m_{1,etas}))$.
- Select r_i as a subset of points from m_1 .
- Generate a proposal model m^* by conditional simulation using r_i as conditioning data. We use DS for multi-point geostatistical simulations.
- Evaluate $L(m^*)$ and accept or reject m^* by the Metropolis acceptance criterion [10].

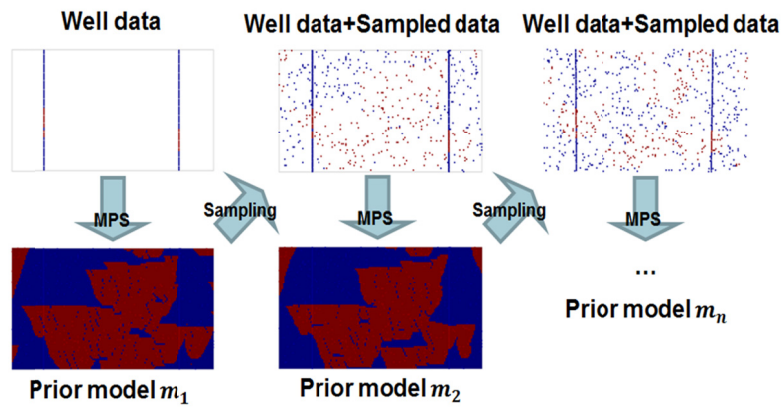


Figure 2 Sketch of the iterative spatial resampling method. An initial model m_1 is randomly sampled to obtain the subset, which is used as conditioning data for generating next prior m_2 . m_2 displays similar local features with m_1 due to the constraints imposed by the conditioning data, and represents a different realization from the prior multi-point geostatistical model.

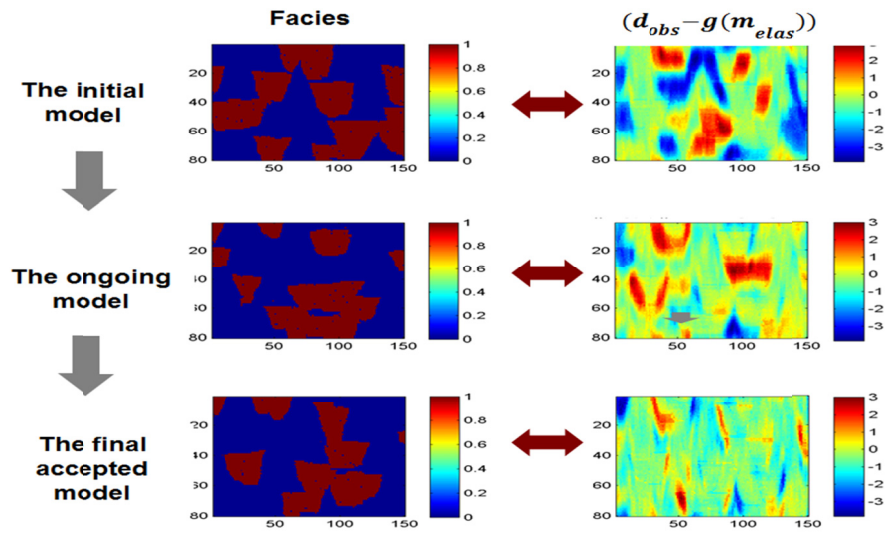


Figure 3 The iteration of a Markov chain using ISR. Left: generated facies models; Right: the residual between seismic data and predicted data from the earth model in each step. This misfit is getting smaller with iterations.

2.2.3. Adaptive spatial resampling

The search strategy of ISR performs successive steps in random directions for exploring various regions of the solution space. Since the search is stochastic, the global minimum will be reached after theoretically, an infinite number of iterations. However, in most practical applications, when the subset conditioning points are selected at random, it can get stuck in a non-optimal local minimum. In this work we improve the efficiency of ISR by adaptive sampling.

At the every iteration, we compare the predicted seismic data with the observed data and thus we have a spatial error map. We can use this information for generating the next step. Instead of just randomly sampling a subset of points to condition the next realization, we adaptively sample important points having lower residual error (see Figure 4). The algorithm probabilistically selects a subset of conditioning points with probability based on the residual error pdf; thus lower error points have a higher chance to be accepted as a conditioning point. Adaptive Spatial Resampling (ASR) accelerates to reach the posterior distribution and efficiently finds an optimal model consistent with the given data. The adaptive selection algorithm should be varied depending on a type of seismic data. Inverted acoustic impedance data in depth can be compared with predicted data directly to calculate a residual error map as shown in Figure 4.

However, since seismograms are recorded in time, direct comparison between data and prediction can be misleading because of timeshifts. Two seismograms in Figure 5 show similar local features at CDP 20; however, since the seismic reflections are not exactly overlapped in time axis, directly subtracted residual error is still high regardless of similarity of underlying facies. Thus, we propose using trace-to-trace cross correlation coefficients to guide the probability of selection. Higher correlation coefficient assigns a higher chance to be accepted as a conditioning location for next step.

Performance of ASR can be sensitive to input parameters such as fraction of selected conditioning points and number of trace locations in a seismogram section. The fraction of subset points controls iteration steps for searching the next better model. A large fraction of conditioning points makes too small a progress at every iteration step while a small fraction can move in relatively large steps but it may lose a spatial structure of previous model. Optimal fraction can be varied depending on the problems. We tested the sensitivity to this parameter and found that adaptive resampling with 1% proportion performs slightly better than the other values (top, Figure 6). In this figure, we can find that retaining a large fraction rapidly reduces root mean square error (RMSE) at the beginning but it gets stuck in a local minimum after 100 iterations. In contrast, chains with 1% fraction move relatively slower but can

reach lower RMSE. The number of selected traces is also an important parameter. More traces account more horizontal spatial structures while it may lose vertical information in the seismic trace since fewer points are selected per trace. Even though we assign the same 1% fraction, the number of traces can affect efficiency of the Markov chain. The bottom Figure 6 is a sensitivity test within our dataset, and it shows 8 trace locations with 1% fraction rate are relatively suitable in this case.

Mosegaard and Tarantola [11] indicate that their sampling method can also be used for optimization, creating a chain of ever-improving realizations by only accepting a proposed model if the likelihood improves. Depending on the acceptance/rejection criterion in the Markov process, it is possible to obtain a chain of realizations aimed to characterize a certain posterior distribution with Metropolis sampling. In the studied cases, ASR yields posterior distributions reasonably close to the ones obtained by rejection sampling, but with important reduction in CPU cost.

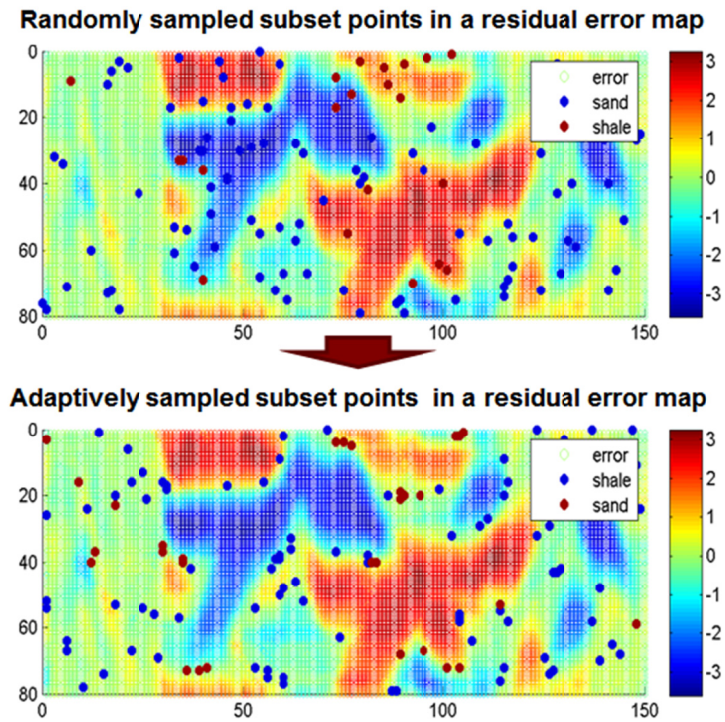


Figure 4 Sampling algorithm of the subset points in the ASR. Background green zone is the low residual points while both red and blue have higher error. In the residual error map, randomly sampled points (top) are located in both low and higher error zone while adaptive sampling subsets (bottom) are located preferentially in low error zone.

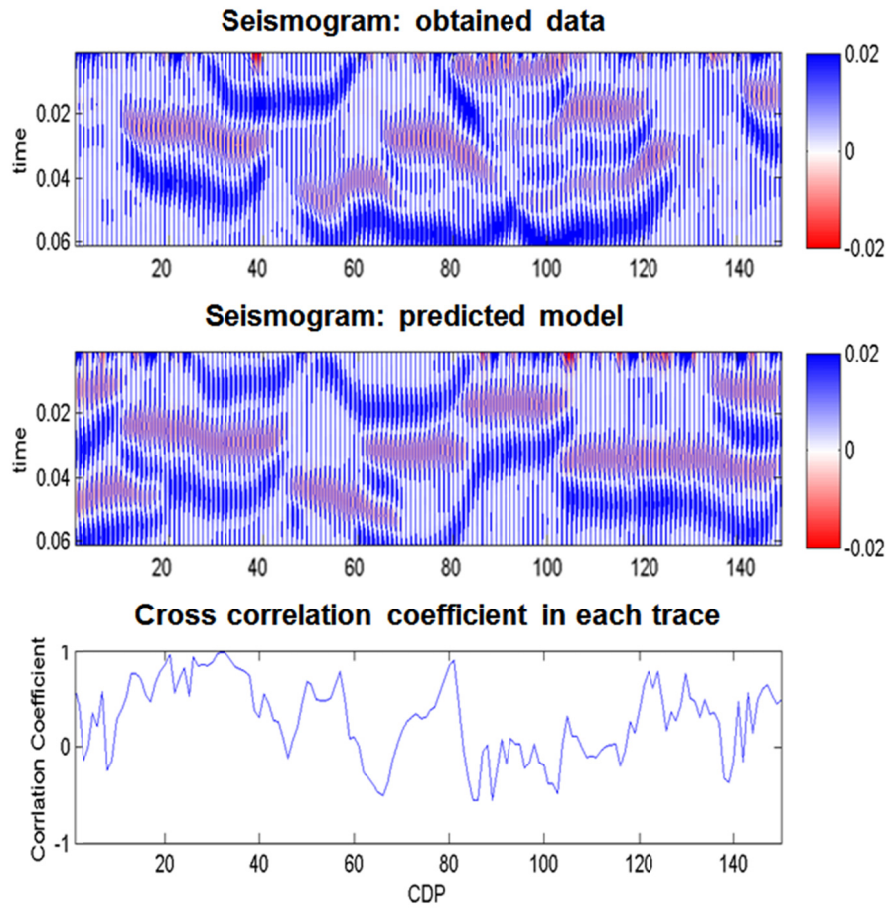


Figure 5 Subset sampling algorithm for seismogram in the ASR. Since the seismogram is traces consisted of wiggles in travel time, directly subtracted variability can miss similar local feature. We used cross correlation coefficients between each trace for adaptive sampling of subset points. The location of a trace having high correlation coefficient with the corresponding data trace has more chance to be selected as subset points for conditioning the next iteration in the chain.

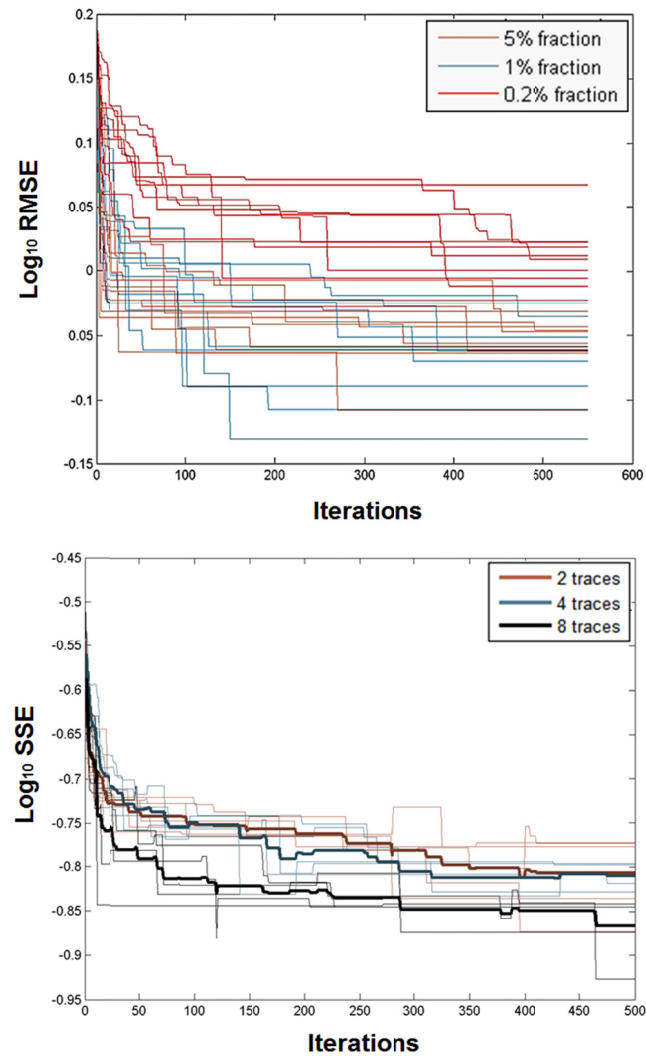


Figure 6 Performance assessment for testing different parameters. Top: adaptive resampling with 1% fraction of conditioning subset points performs slightly better than the other values, but this can be different depending on the problem; Bottom: The sensitivity of the number of traces is tested. 8 traces case was an ideal setting in this study.

3. Test case

3.1. Synthetic Dataset

Synthetic 2D facies and seismic dataset are presented to demonstrate the validity of the proposed inversion technique. The two-dimensional models used were extracted from a modified version of the top layer of the Stanford VI synthetic reservoir. The Stanford VI reservoir [6] was created by the geostatistics group at Stanford University to test algorithms. All the information about the model relevant to this work is summarized in Figure 7. The reference facies model is a sand-shale channel system with 80 cells in the vertical (z) direction ($dz = 1\text{m}$) and 150 cells in x ($dx = 25\text{m}$).

We show the use of ASR for two types of seismic data. One is where we have P-impedance inverted from the seismic section (say from a conventional impedance inversion), and we use the impedance as an attribute for the stochastic lithofacies inversion. The second is where the seismic data are the normal-incidence seismograms themselves, before inversion for impedance. Using appropriate rock physics models for the sand and shale, we compute acoustic impedance from the P-wave velocities and densities. We applied a frequency-domain Born filter for surface seismic reflection geometry with a 5~50 (Hz) bandwidth. This is the forward model for the impedance data type. For the second case to generate a reference normal-incidence seismic section, we assumed convolutional seismic forward modeling without noise and applied a 50 (Hz) wavelet. For the inversion process, we assumed that we have only the acoustic impedance data or the seismogram section, two wells with log information, and a training image.

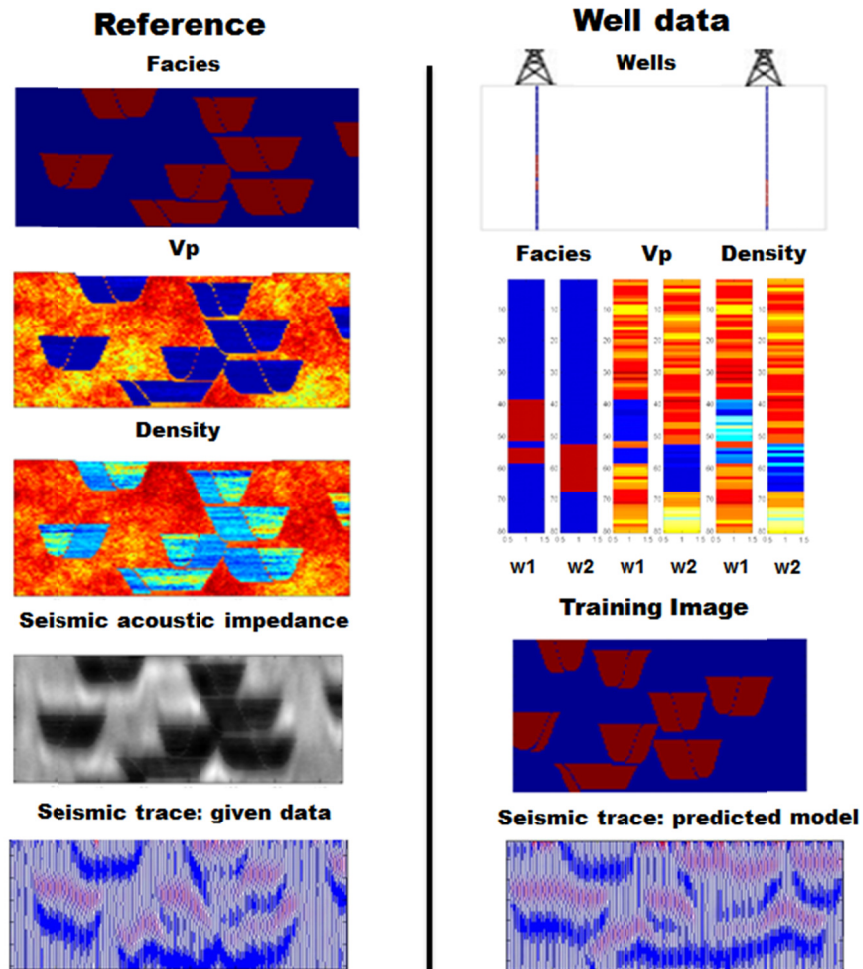


Figure 7 Left: The spatial distribution of the facies, P-wave velocities (V_p) and densities (ρ) are assumed as the reference. The filtered seismic band acoustic impedance and normal-incidence seismogram are at bottom left. Right: The data of two wells are given as above and the wells are located at CDP25 and CDP125, respectively. Training image for MPS is shown at the bottom of the right column.

3.2. Results

First, we generated multiple prior spatial models using multiple-point geostatistical algorithm and these are used to find posteriors by rejection sampling. Rejection sampling method is one perfect way to represent posterior pdf. However, since it requires a large number of evaluations of forward model, it is inefficient. Figure 8 shows the results as the reference and the E-types (ensemble averages) of models. Since the hard data comes from two wells, the E-type map of priors shows its limitation of lateral resolution. Rejection sampling is accomplished to represent posterior pdf as the reference. We tested ISR and ASR as equivalent sampling methods by comparing their results with rejection sampler.

3.2.1. Case 1: acoustic impedance for lithofacies characterization

When we used acoustic impedance data as the seismic attribute, both rejection sampler and ASR found clear channel distribution and these results look the same while ISR found similar channel distribution with ambiguity (first row of the Figure 9). However, the result of rejection sampler is the average of 125 accepted models after evaluating 100,000 prior models while ASR with Metropolis algorithm uses 1 Markov chain with 500 iterations (94 posteriors sampled in ASR and 25 posteriors sampled in ISR). ASR shows significantly better efficiency when compared to rejection sampling. The root mean square errors (RMSE) versus iterations for the 10 Markov chains are also shown in Figure 10 for comparing the predictability of ISR and ASR. ASR chains reached lower error zone more rapidly than ISR chains.

3.2.2. Case 2: seismograms for lithofacies characterization

Since seismogram data has more uncertainty than acoustic impedance due to the wavelet effect and time shifts, the predictability of sampling algorithm is critical in this case. The performance of ISR and ASR are compared in bottom of Figure 9, and it shows a big difference in the E-type result. ASR found similar channel distribution as rejection sampler while ISR lost channels away from wells (ISR sampled 25 posteriors sampled in a chain). ASR sampled 51 posteriors in 1 Markov chain with 500 iterations

while rejection sampler accepted 140 posteriors among 100,000 priors. Variance map (bottom figure in each section) shows that ASR captures the range of uncertainty fairly well as compared with rejection sampler. Distance-based representation using multi-dimensional scaling (MDS) in Figure 11 also shows that the samples from ASR are distributed near the reference with the posteriors from rejection sampling. Thus we can conclude that ASR can be a fair approximation of rejection sampler. Since our reference is located away from the most of priors, rejection sampler is inefficient for find posterior models. Sampled posteriors by ISR could not reach the whole posterior distribution yet. Hence, ASR can be used as an efficient posterior sampler.

3.2.3 Case 3: Finding facies not seen in well data

In this case, we assume one oil sand distribution away from the two well locations. We have seismogram data, well logs without oil sand information, and a training image (see Figure 12). For this task, we applied realistic rock physics relationship from actual well logs, and generated oil sand properties from the brine sand properties at the wells using Gassmann's equation [2]. Figure 12 shows rejection sampler and ASR results as probability maps. Rejection sampler found nearly correct distribution compared to the reference after 50,000 evaluations while ASR found similar distribution using one chain of 1,000 evaluations. In more realistic task, ASR also shows its applicability as a fair and efficient sampler.

3.2.4. ASR as an optimizer

As an optimizer the performance of ISR and ASR are compared in Figure 13. Here our objective is to find optimal models which match the given seismic data. The average of 30 chains as a thick line in Figure 13 shows the efficiency of ASR. Especially in the early stage of iterations, ASR moves quickly to find a better model while ISR goes down slowly with long flat sections. On average ASR can manage to find models with much lower rms error. The efficiency can be compared by the number of iterations required to reach the same logarithm RMSE; the value of ISR at the 500th iteration averaging over 30 chains was the same as the result of the 27th iteration for ASR.

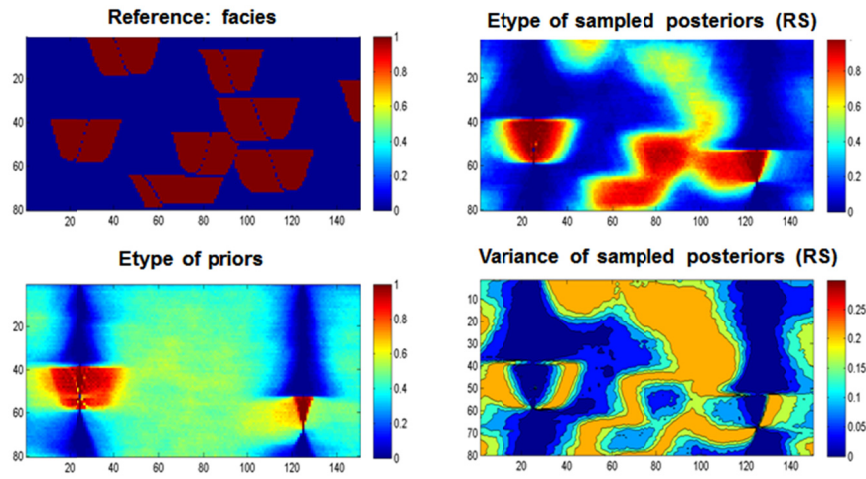
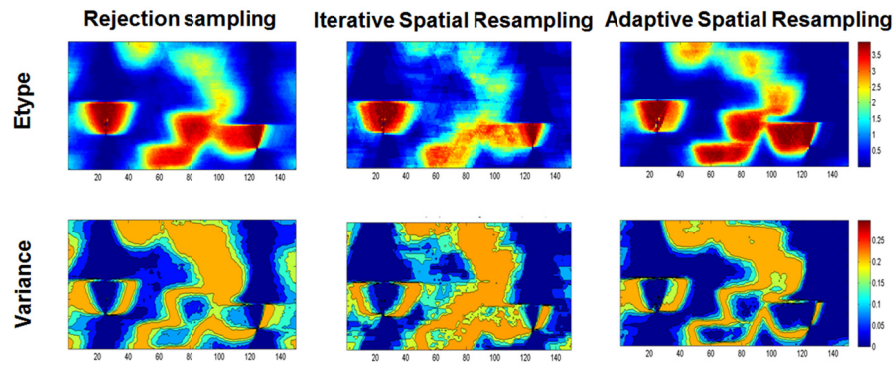


Figure 8 Representation of the averages of ensembles of models. Top: (left) the reference facies and averaged prior models; (right) the E-type of rejection sampling results and its variance.

1. Acoustic Impedance



2. Seismogram

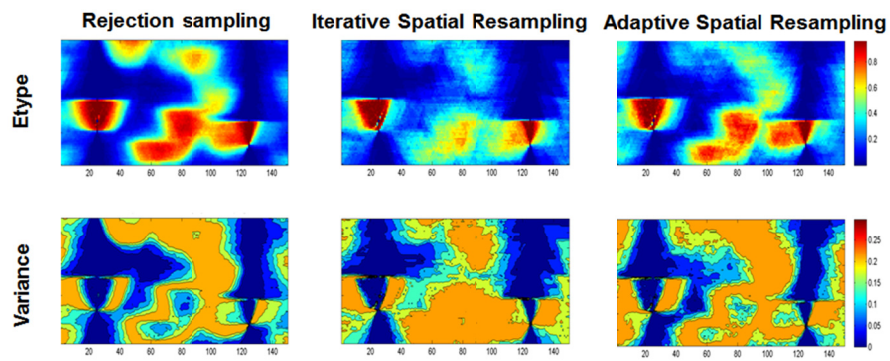


Figure 9 Representation of the averages of ensembles of models. Top: (first row) the E-type of rejection sampling results, ISR and ASR using acoustic impedance as the obtained data; (second row) the variance of each algorithm, respectively. Bottom: (first row) the E-type of rejection sampler, ISR and ASR using seismogram section as the obtained data, and (second row) its variance. Within limited evaluations, ASR show similar E-type and variance map compared with the result of rejection sampling in both cases.

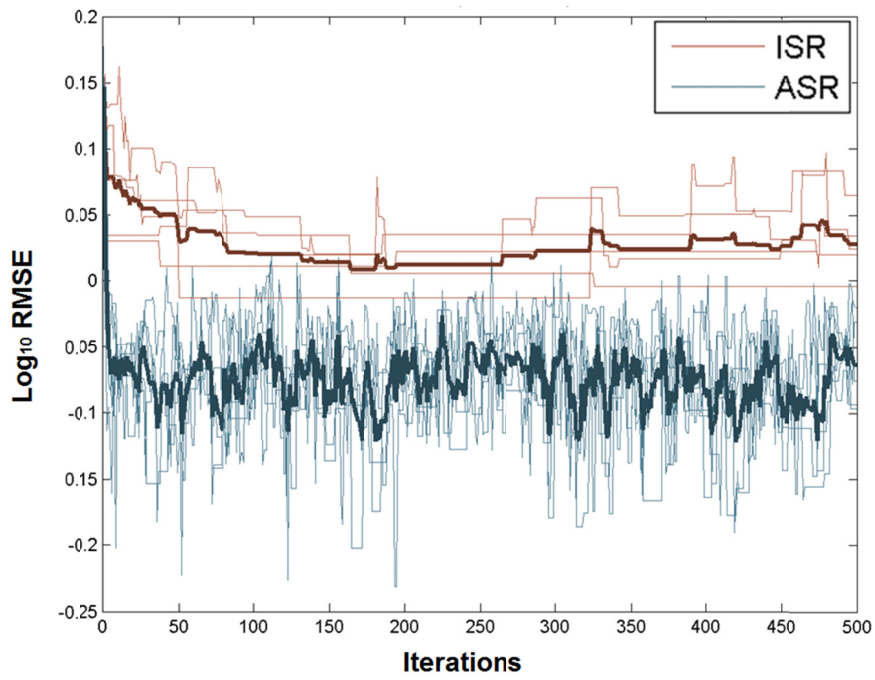


Figure 10 Adaptive spatial resampling (blue curves) and iterative spatial resampling (red curves) are compared as a posterior sampling method for 5 Markov chains. The average of 5 chains for each case is shown as a thick line. ASR chains reaches reached lower error zone more rapidly and lively samples the posteriors.

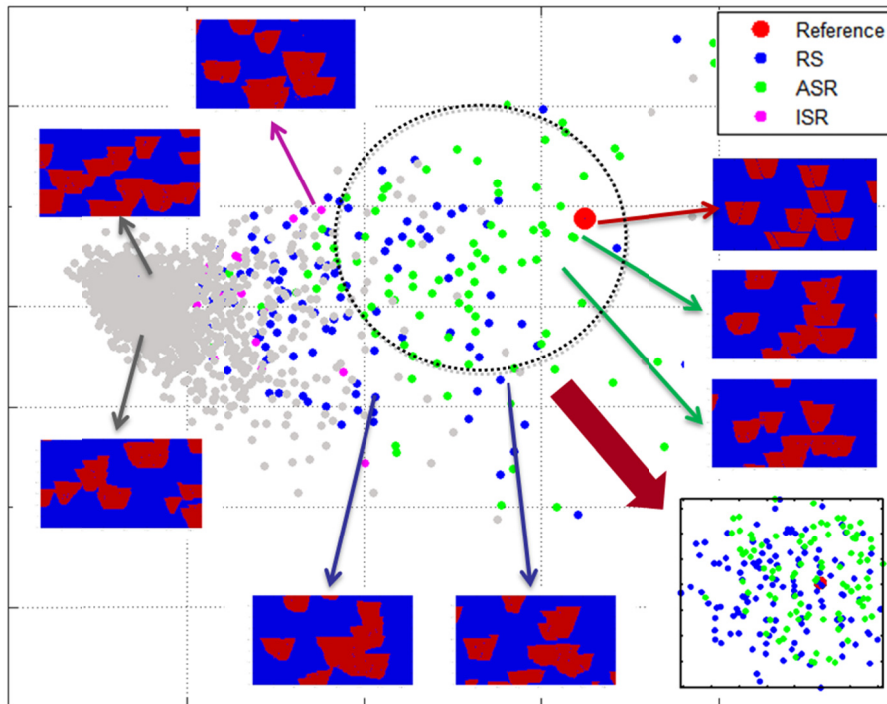


Figure 11 Multi-Dimensional Scaling (MDS) projection of all models. The gray points are prior models and the red point is the reference. The blue are the posteriors by rejection sampling and they are clustered around the true model. ASR and ISR results are shown by green and magenta points, respectively.

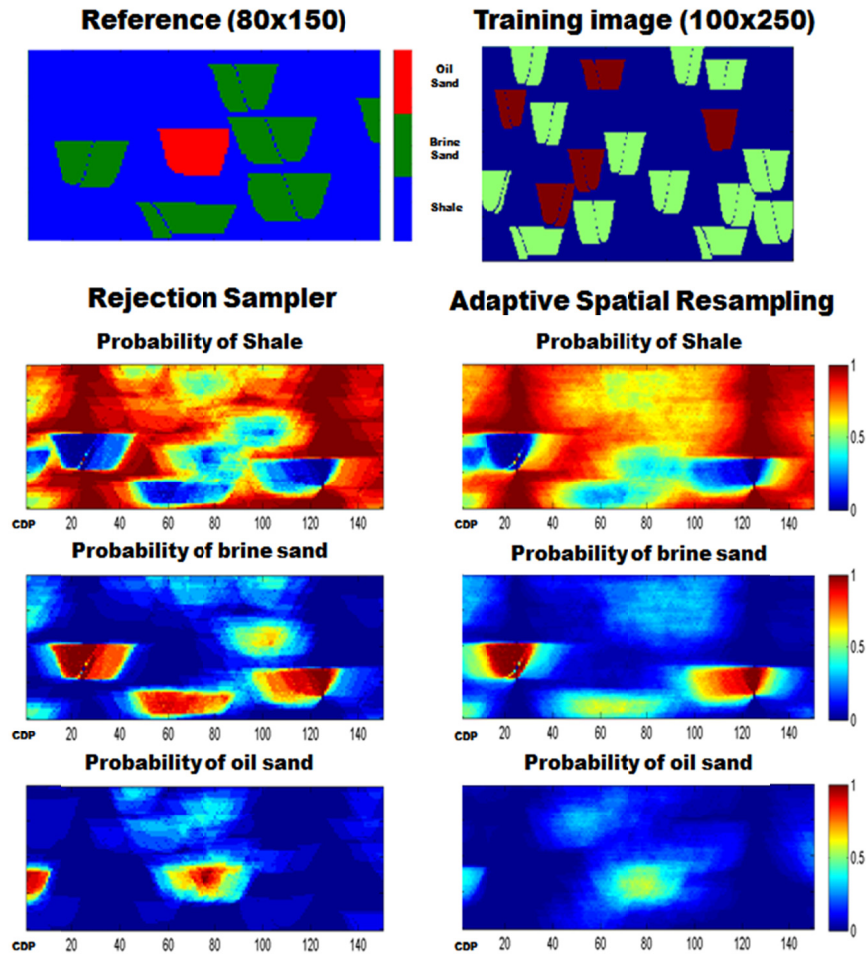


Figure 12 A case study for detecting oil sand distribution away from wells, when wells do not have any oil sand. : Representation of the averages of ensembles of models. Top: (left) the reference three facies and (right) a training image; Bottom: (left) the probability map of rejection sampler in each facies and (right) the probability map of the posteriors sampled by ASR. Within relatively limited evaluations, ASR show similar probability map compared with the result of rejection sampler.

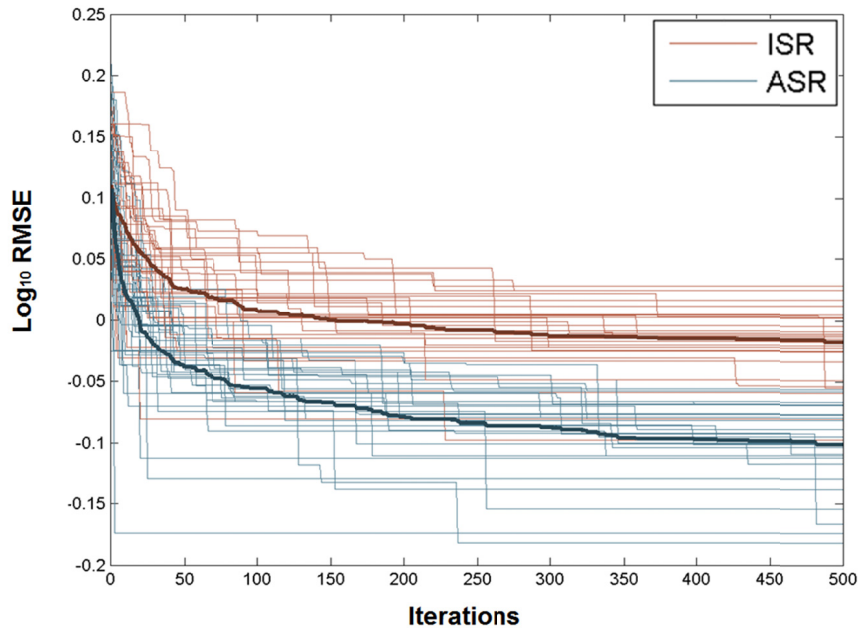


Figure 13 Adaptive spatial resampling (blue curves) and iterative spatial resampling (red curves) are compared for 30 Markov chains. ASR as an optimizer was faster to find out the most likely models, and found models with lower rms error. The average of 30 chains for each case is shown as a thick line. ASR rapidly reduced the residual error especially in the early stage of iterations.

4. Conclusions

We presented the Adaptive Spatial Resampling method (ASR) for seismic inverse modeling. ASR perturbs realizations of a spatially dependent variable while preserving its spatial structure. ASR also accelerates the sampling efficiency without decreasing range of uncertainty by making use of the residual error at each step of the chain to condition the next step. In the studied cases, it yields posterior distributions reasonably close to the ones obtained by rejection samplers, with important reduction in time and

computing cost. Thus ASR is suitable for conditioning facies models or characterizing reservoir properties to spatially distributed seismic data.

Depending on the acceptance/rejection criterion in the Markov process, it is possible to obtain a chain of realizations aimed either at characterizing a certain posterior distribution with Metropolis sampling or at calibrating one realization at a time. This study will be applied in actual field data as future task.

5. Acknowledgment

The authors thankfully acknowledge the sponsors of the Stanford Center for Reservoir Forecasting (SCRF).

Bibliography

- [1] Arpat, B. G., 2005, Sequential simulation with patterns: Ph.D. dissertation, Stanford University.
- [2] Avseth, P., T. Mukerji, and G. Mavko, 2005, Quantitative seismic interpretation, applying rock physics to reduce interpretation risk: Cambridge University Press.
- [3] Bosch, M., L. Cara, J. Rodrigues, A. Navarro, and M. Diaz, 2004, The optimization approach to lithological tomography: Combining seismic data and petrophysics for porosity prediction: *Geophysics*, 69, 1272-1282.
- [4] Bosch, M., 1999, Lithologic tomography: From plural geophysical data to lithology estimation: *Journal of Geophysical Research*, 104, 749-766.
- [5] Bosch, M., T. Mukerji, and E.F. Gonzalez, 2010, Seismic inversion for reservoir properties combining statistical rock physics and geostatistics: A review, *Geophysics*, 75, no 5, 165-176
- [6] Castro, S, J. Caers, and T. Mukerji, 2005, The Stanford VI reservoir: 18th Annual Report, Stanford Center for Reservoir Forecasting, Stanford University.
- [7] Gonzalez, E. F., T. Mukerji, and G. Mavko, 2008, Seismic inversion combining rock physics and multiple-point geostatistics: *Geophysics*, 73, no. 1, R11-R21.
- [8] Mariethoz, G., P. Renard, and J. Caers, 2010a, Bayesian inverse problem and optimization with iterative spatial resampling, *Water Resources research*, 46, W11530.
- [9] Mariethoz, G., P. Renard, and J. Straubhaar, 2010b, The direct sampling method to perform multiple-points geostatistical simulations, *Water Resources Research*, 46, W11536.
- [10] Metropolis, N., et al., 1953, Equation of State Calculations by Fast Computing Machines: *Journal of Chemical Physics*, 21, 1087-1092.
- [11] Mosegaard, K., and A. Tarantola, 1995, Monte Carlo sampling of solutions to inverse problems: *Journal of Geophysical Research*, 100(B7), 12, 431-447.
- [12] Mukerji, T., P. Avseth, and G. Mavko, I. Takahashi, and E. F. Gonzalez, 2001a, Statistical rock physics: Combining rock physics, information theory, and geostatistics to reduce uncertainty in seismic reservoir characterization:

The Leading Edge, 20, no. 3, 313-319.

- [13] Mukerji, T., A. Jorstad, P. Avseth, G. Mavko, and J. R. Granli, 2001b, Mapping lithofacies and pore-fluid probabilities in a North Sea reservoir: Seismic inversions and statistical rock physics: *Geophysics*, 66, 988-1001.
- [14] Strebelle, S. B., and A. G. Journel, 2001, Reservoir modeling using multiple point statistics: Society of Petroleum Engineers, 71324.
- [15] Tarantola, A., 1987, Inverse problem theory: Methods for data fitting and model parameter estimation: Elsevier Scientific Publ. Co., Inc.
- [16] Tarantola, A., 2005, Inverse problem theory and methods for model parameter estimation: SIAM.